

Tunnelling and Coherence of Mesoscopic Spins

Single Molecule Magnets allow studies at the border between the classical and quantum regimes.

Bernard Barbara

Mesoscopic physics is a sub-discipline of condensed-matter physics that focuses on the properties of solids in a size range intermediate between bulk matter (macroscopic) and individual atoms (microscopic). In particular, it is characteristic of a domain where a large number of particles can interact in a quantum-mechanically correlated fashion. In this article, it is shown that the collective spins of large and complex magnetic molecules can be tuned between their classical and quantum regimes thus enabling studies at the border of the two.

The possibility (or impossibility) of observing quantum phenomena at the macroscopic scale has been discussed from the earlier times of quantum mechanics (see, for example the Schrödinger's cat paradox [1]). Experimental studies on "macroscopic quantum tunnelling" likely started in the 70s or 80s, in particular under the impulse of A. J. Leggett [2]. The first solid-state observation of tunnelling at the macroscopic scale was apparently done on micrometer-size Josephson junctions at IBM Yorktown Heights in 1981. It was shown that the "switching current" of a junction, thermally activated at high temperature, becomes independent of temperature below a certain crossover temperature, in agreement with the expectations of quantum tunnelling where the barrier is passed at constant energy. In magnetism, the initial idea was to observe whether the reversal of the magnetization of magnets, thermally activated at high temperature, could take place by quantum tunnelling at low temperature – the barrier is due to the magneto-crystalline anisotropy energy, which fixes two equivalent spin directions, up or down. Studies on rare-earth-based magnets and their extensions to nanomagnetic systems showed that the "switching field" at which the magnetization reverses becomes independent of temperature when it is lowered, suggesting a crossover between thermal activation and tunnelling similar to that of the Josephson junctions [3]. However, this conclusion was rather ambiguous due to the presence of distributions (particle sizes, energy barriers, switching fields ...). This led us to start two parallel projects using "micro-SQUIDS" for single-particle measurements and "identical magnetic nanoparticles" for ensemble measurements.

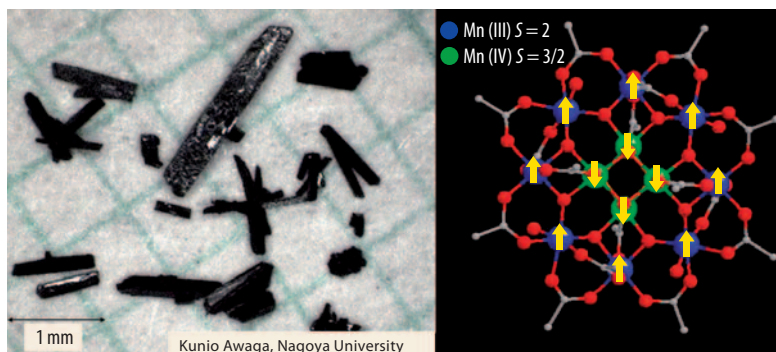


Fig. 1 Single crystals of the molecule Mn_{12} -ac can be considered as macroscopic quantum magnets (left). The complex Mn_{12} -ac molecule (right) contains several hundred particles (electrons and atoms) that participate in the construc-

tion of the collective spin $S = 10$ equal to the vector sum of eight spins 2 and four spins $3/2$. In this schematic view only manganese ions and some oxygen atoms are represented [4].

This short article will focus on the second aspect. The nanoparticles which were used are the so-called Single Molecule Magnets (SMMs). SMMs are identical magnetic molecules well isolated from each other and forming the motif of a lattice. In general their symmetry is uniaxial and their magnetic moment comes from 3d transition ions coupled with each other by strong intramolecular super-exchange interactions. The absence of intermolecular exchange pathways shows that the SMMs can be considered as magnetic nanoparticles interacting through long-range dipolar interactions only. The archetype and most popular SMM is the so-called Mn_{12} -Acetate (Mn_{12} -ac) molecule with formula

IN BRIEF

- In Single Molecule Magnets (SMMs) like Mn_{12} -ac, quantum tunneling enables spin reversal, even at low temperatures where thermal activation is blocked.
- As a consequence the hysteresis loop of SMMs is constituted of several plateaus and steps.
- SMMs have been proposed as candidates for magnetic data storage and for quantum computation applications.
- In general, the field of "mesoscopic quantum spin dynamics" is developing in different directions, e. g. molecular spintronics, spin-based quantum computation and mechanisms of decoherence, with extension to more complex or simpler systems.

Dr. Bernard Barbara, Institut Néel, CNRS, 25 rue des Martyrs, BP 166, 38042 Grenoble cedex 9, France. Plenary talk given on the occasion of the conferment of the Gentner-Kastler Prize at the DPG conference in Berlin.

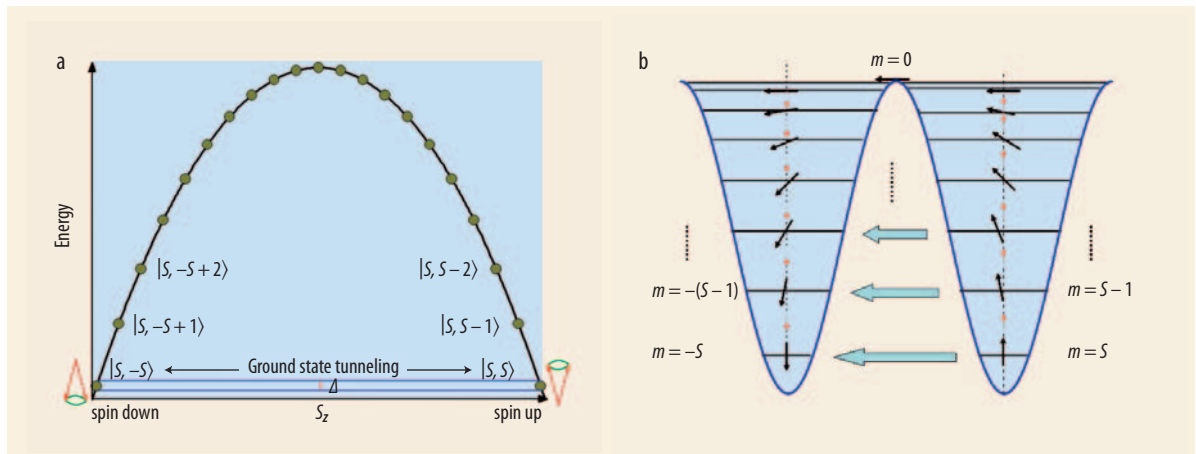


Fig. 2 (a) Zero-field-energy spectrum $E(m)$ of Hamiltonian (1) represented vs. the molecule spin projection $m = \langle S_z \rangle$. The parabolic anisotropy energy maximum at $m \approx 0$ (classical spin perpendicular to the anisotropy axis) and minimum at $m = \pm S$ (up and down classical spin parallel to the anisotropy axis) is a quantum representation of the classical energy

barrier. For clarity, the tunnel splitting Δ is schematically represented only for the ground state. The tunnelling states $|S\rangle$ and $|-S\rangle$ are connected through the rising or descending operators, which modify the value and change the sign of $m = \langle S_z \rangle$. The excited intra-well “semi-classical” states are connected to each other by spin-phonon transitions.

(b) A more popular representation of the same energy barrier and “ladder-like” level scheme $E(\theta)$ where $\theta = \cos^{-1}(m/S)$, with $0 \leq \theta \leq \pi$, is the quantized tilt-angle associated with the precession of \mathbf{S} in each well. The large blue arrows indicate tunnelling whereas the thin red ones indicate spin-phonon transitions for thermal activation.

$[\text{Mn}_{12}\text{O}_{12}(\text{OAc})_{16}(\text{H}_2\text{O})_4] \cdot 4\text{H}_2\text{O} \cdot 2\text{AcOH}$ (Fig. 1) and $S = 10$. Synthesized more than 20 years ago by Lys [4], this molecule became popular in the 90s during the explosion in interest in nanomagnetism.

Classical versus quantum-mechanical hysteresis

The SMM spin $\mathbf{S} = \sum \mathbf{S}_i$, sometimes called the “collective spin”, corresponds to the ground-state spin of the molecule (the vector summation is over all the magnetic ions with elementary spins \mathbf{S}_i). A strong uniaxial crystal-field anisotropy compels all the molecule spins, and therefore \mathbf{S} , to be parallel (or anti-parallel) to the crystallographic c -axis. Under the application of an anti-parallel magnetic field, \mathbf{S} should switch and orient parallel to the field. In the classical option this is done in a single-step rectangular magnetization-field hysteresis loop with a switching field equal to the anisotropy field $H_A = 2K/M_s$ (where K measures the crystal-field anisotropy energy, $M_s = g\mu_B S$ is the SMM magnetic moment, μ_B the Bohr magneton and g the Landé factor). In $\text{Mn}_{12}\text{-ac}$, H_A is very large, ensuring good stability of the states $\pm S$ along the c -axis [5].

It is because of this bi-stability that SMMs have been proposed as potential candidates for high-density magnetic recording elements. We will see below that the tiny size of these magnets (a few nanometers) gives them a strong quantum character, which also makes them candidates for quantum computing applications. This led to a rapid growth in research ending in the discovery of hundreds of new SMMs. This research in molecular and supramolecular chemistry (SMMs self-organize in bottom-up approaches) is still very active.

As the SMM spin generally results from symmetrical exchange interactions, the different spin states S , S

$-1 \dots$ are not coupled with each other. As a consequence the dynamics involves a single energy barrier, the one associated with the lowest ground-multiplet S . The corresponding $(2S + 1)$ degeneracy is removed by the crystal-field leading to an ensemble of Ising doublets $\pm S$, $\pm(S - 1) \dots$. The uniaxial anisotropy manifests itself by a “separation” of each one of the doublets spin components, which therefore “cannot see each other” (Fig. 2a). As a consequence these spins can reverse only by successive spin-phonon transitions going through the top of the barrier (thermally activated reversal), unless the crystal field is not fully axial and contains non-Ising (transverse) terms. These last terms couple those spin-up and spin-down states across the barrier that are in coincidence, leading to quantum tunnelling. As we will see below, this is generally the case showing that if the temperature is low enough to prevent spin reversal by thermal activation, spin reversal can still occur by quantum tunnelling (Fig. 2). More precisely, when lowering the temperature the $m = 0$ state becomes inaccessible and only the lowest states $m = S - 1$, $m = S - 2 \dots$ can be thermally activated, allowing quantum tunnelling if these states are in coincidence with empty states of opposite spins in the next well as shown in Fig. 2b (zero-field) and Fig. 3 (finite field). This “thermally activated tunnelling” regime is followed at low temperature and down to zero Kelvin (below a crossover temperature T_c) by ground-state tunnelling spin reversal from $m = S$ to $-S$ (zero-field) or from $m = S$ to $-(S - 1)$, $-(S - 2) \dots$ (finite field). The $\text{Mn}_{12}\text{-ac}$ SMM is the first magnetic object that showed unambiguously such mesoscopic quantum tunnelling effects [6, 7]. Owing to the fact that these molecules are identical and interact only weakly, ensemble measurements on a single-crystal were sufficient.

The hysteresis loop of $\text{Mn}_{12}\text{-ac}$ (and generally of SMMs single crystals) is constituted of plateaus and

steps (Fig. 4). Nothing happens in the plateaus where spin-tunnelling is forbidden, the levels in the two wells not being in coincidence but in staggered rows. On the contrary each step, associated with a coincidence of the two “ladder-like” series of levels, corresponds to a temperature-independent switching field at which the magnetization reverses partially by tunnelling (only a fraction of the total number of molecule spins reverses, see below) (Fig. 4). Completely different from the classical single-step hysteresis loop, the staircase hysteresis loop of Mn₁₂-ac is fully independent of temperature below T_c (at the Kelvin scale) and shows full magnetization reversal in fields much smaller than H_A , invalidating completely the classical option, although hysteresis – on which permanent magnets are based – may be considered as the most typical example of classical phenomena.

Microscopic description

The general form of the microscopic Hamiltonian of a SMM multiplet S is of the type $H = \sum J_{ij} \mathbf{S}_i \mathbf{S}_j + \sum D_i (\mathbf{n}_i \mathbf{S}_i)^2 + \dots$ where summations are performed over all the SMM spins ($i, j = 1 \dots N = \text{total number of spins of the SMM}$). The first term describes intra-molecular Heisenberg pair couplings and the other ones the single-ion anisotropy terms deriving from a crystal field whose local energy minima are along unit vectors \mathbf{n}_i related to the local symmetry of each spin site (\mathbf{n}_i are generally nearly parallel to the molecule c -axis). The

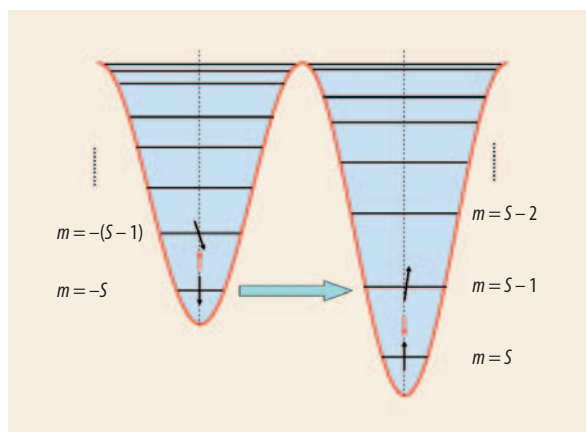


Fig. 3 The double-well energy barrier in a magnetic field parallel to the spin-up direction after a selection of down spins (before tunnelling, only the left well is occupied). When the field increases from zero the left ladder-like level scheme shifts upward whereas the right one shifts downward, allowing a succession of resonances. The figure corresponds to the first tunnel resonance ($n = 1$) from $|m = -S\rangle$ to $m = |S - 1\rangle$ (at low temperature only the ground-state $|m = -S\rangle$ is occupied). This resonance follows the zero-field resonance ($n = 0$), explaining why the state $m = |S\rangle$ is occupied. The second resonance ($n = 2$) will correspond to the coincidence of $m = -|S\rangle$ with $m = |S - 2\rangle$. At finite temperature, spin-phonon transitions (red arrows) populate the state $-|S - 1\rangle$, allowing $-|S - 1\rangle \rightarrow |S - 2\rangle$ thermally activated tunnelling. After tunnel escape the excited spins of the right well become fully parallel to the applied field by joining the ground state through intra-well phonon emission (red arrows).

Hilbert space dimension $D_H = (2S + 1)^N$ is generally too large to allow exact diagonalization unless approximations are made to reduce it. The Hilbert space dimension of Mn₁₂-ac, $D_H = (2 \times 3 / 2 + 1)^4 (2 \times 2 + 1)^8 = 10^8$ (each term is for one spin species, see Fig. 1) can be lowered to $D_H = 10^4$ if the spin pairs with the largest couplings J_{Max} are “locked”, i. e. form a single spin equal to the algebraic sum of the two. Exact diagonalization can then be performed giving access to all the energy levels at energy below J_{Max} . Another, more drastic approximation consists in taking an effective or “collective” Hamiltonian in which, not only a pair, but all the spins are locked forming the collective SMM spin S . In this case, the first term in the Hamiltonian disappears, and only the crystal-field terms remain with the global symmetry of the molecule i. e. with longitudinal (Ising) and transverse (non-Ising) terms. In the case of Mn₁₂-ac this Hamiltonian (limited to the 4th order terms) can be expressed vs. usual spin operators:

$$H = -DS_z^2 - BS_z^4 - C(S_z^4 + S_x^4) - g\mu_B\mu_0\mathbf{S}\mathbf{H}. \quad (1)$$

The quantization z -axis coincides with the tetragonal c -axis of the molecule. With $S = 10$, the Hilbert dimension $D_H = 2S + 1 = 21$ is here sufficiently small for easy diagonalization and at the same time it constitutes an excellent approximation for the lowest multiplet S , the energy level spectrum of which is fully consistent with the one issued from exact diagonalization in the $D_H = 10^4$ case. This type of “collective spin Hamiltonian”, first used with Mn₁₂-ac, proved to be valid for most SMMs discovered afterwards.

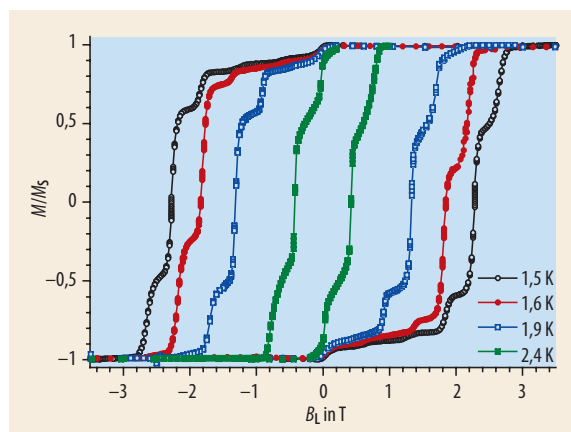


Fig. 4 Hysteresis loops of the reduced magnetization M/M_S vs longitudinal magnetic field B_L measured at different temperatures in a single crystal of Mn₁₂-ac. This staircase shape comes from a succession of plateaus where the magnetization is nearly constant, especially at low temperature where the thermal activation is blocked. The plateaus extend over field ranges where the spin-up and spin-down level structures (ladder-like) are not in coincidence (no resonance). The steps with fast magnetization reversal correspond to the resonance fields. At each step the spin of a finite fraction of Mn₁₂-ac SMM reverses by quantum tunnelling and aligns parallel to the applied field. Hysteresis loops become narrower by the effect of “thermally activated tunnelling” when the temperature increases. These observations at the border of classical physics (presence of broad hysteresis loop) and quantum physics (tunnelling) are quantitatively explained solely on the basis of the quantum theory.

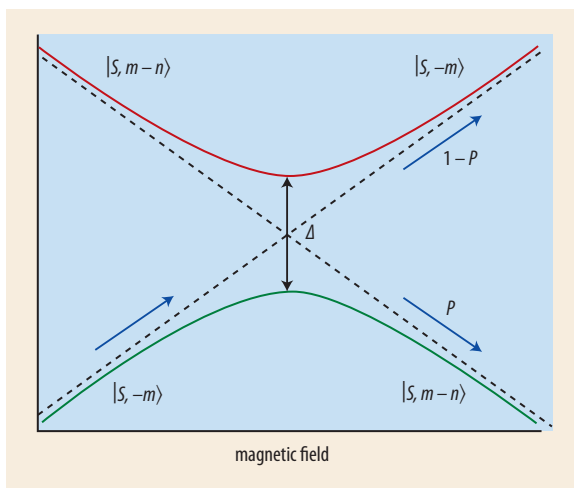


Fig. 5 Energy E vs. magnetic field H near an avoided level crossing with tunnel splitting Δ . The “classical” barrier separating the states $\pm|S_z\rangle$ intervenes here in the value of Δ only, reducing it exponentially. The slope dE/dH represents $|S_z\rangle$, and “tunnelling” simply means “stay on the ground state”. This occurs with a certain probability P equal to the Landau-Zener probability for an isolated spin. This simple and beautiful picture of mesoscopic tunnelling is deeply modified by the spin bath resulting from other molecule spins and nuclear spins [8].

The longitudinal (or diagonal) anisotropy terms of (1) with coefficients D and $B \ll D$ give the two ladder-type energy levels separated by a barrier in zero-field $E(m) \approx -Dm^2 - Bm^4$, where $m = \langle S_z \rangle$ is the spin projection on the z -axis (Fig. 2a). The well-known double-well energy barrier can be obtained from this $E(m)$ parabolic barrier by plotting $E(\theta)$, where $\theta = \cos^{-1}(m/S)$ ($0 \leq \theta \leq \pi$) is the quantized tilt angle associated with the precession of \mathbf{S} in each well (Fig. 2). This semi-classical description, valid when the spins of each well “do not see” each other, becomes fully quantum when there is communication between them, i. e. when tunnelling is allowed ($C \neq 0$ and the levels are in coincidence or at “resonance”).

The application of a large magnetic field orienting all the spins selects one of the two $\pm|S\rangle$ ground-states (e. g. $+|S\rangle$). If the field is switched back to zero, the states $+|S\rangle$ and $-|S\rangle$ come to resonance again (Fig. 2) but with nearly 100 % of the molecules with $+|S\rangle$ and almost zero with $-|S\rangle$ (at zero Kelvin). This highly non-equilibrium state will spontaneously evolve towards equilibrium through tunnelling: $2S/4$ successive applications of S^4 will change the ground-state spin from $m = |S\rangle$ to $-|S\rangle$ (each application of this operator changes m in $m - 4$). For a single molecule, equilibration should be approached through back and forth $|S\rangle \leftrightarrow -|S\rangle$ transitions (quantum telegraph noise), whereas for a single crystal equilibration results from the ensemble average having 50 % of the molecules with spins up ($+|S\rangle$) and 50 % with spins down ($-|S\rangle$).

In the presence of an applied longitudinal field $\mu_0 H_z$, the states $|m\rangle$ and $|n - m\rangle$ (with $n \neq 0$) can be set at resonance. The energy of the states with spin projections $\parallel \mu_0 H_z$ will actually decrease and the spin-up, spin-down “ladders” will shift in opposite directions,

allowing successive resonances of the ground-state $-|S\rangle$ (here we have assumed an initial selection of $-|S\rangle$), with $|S - 1\rangle$ ($n = 1$), with $|S - 2\rangle$ ($n = 2$) and more generally with $|S - n\rangle$ with $n \leq S$ (Fig. 3). The magnetic field fulfilling this resonance condition is obtained by equalizing the eigenstate energies $E_S = E_{n-s}$:

$$g\mu_B\mu_0 H_{zn} = nD[1 + (B/D)(S^2 + (S - n)^2)]. \quad (2)$$

Tunnelling reversal occurs at $n = 0$ (zero-field), $n = 1$ (first step), $n = 2$ (second step) ... leading to the hysteresis loop of Fig. 4. The steps are almost equally separated because $B \ll D$ (the approximation $g\mu_B\mu_0 H_{zn} \approx nD$ is often used). Each one of these $\mu_0 H_{zn}$ is the temperature-independent switching field for tunnel spin rotation. In between the $\mu_0 H_{zn}$ there is no coincidence (the two ladders are shifted with each other, giving staggered rows), tunnelling is impossible and the magnetization remains constant leading to hysteric plateaus (Fig. 4).

The tunnelling rate at zero Kelvin – i. e. the number of tunnelling events per second in a crystal – and therefore the size of the steps is proportional to the probability for $|S\rangle \rightarrow |n - S\rangle$ tunnelling events issued from the ground state. The tunnelling rate $\Gamma_{S, n-s} \propto \Delta_{S, n-s}^2$ is proportional to the square of the tunnel splitting $\Delta_{S, n-s}$ removing the degeneracy of the states $|S\rangle$ and $|n - S\rangle$ under the effect of off-diagonal terms C in (1) (Fig. 5). The proportionality coefficient depends strongly on the case which is considered: the isolated single-molecule or an ensemble of weakly interacting molecules.

For a single-spin the zero Kelvin tunnelling rate is proportional to the tunnel probability obtained from exact diagonalization of the time-dependent Schrödinger equation of the two (tunnelling) states $|S\rangle$ and $|n - S\rangle$ (this is an application of the well-known Landau-Zener model, Fig. 5). This ground-state tunnelling probability is expressed as:

$$P_{LZ} = 1 - \exp[-\pi(\Delta/\hbar)^2/\gamma c] \sim \pi(\Delta/\hbar)^2/\gamma c \ll 1, \quad (3)$$

where $c = \mu_0 dH_z/dt$ is the sweeping field velocity, $\Delta = \Delta_{S, n-s}$ and $\gamma = g\mu_B/\hbar$ the gyromagnetic factor (\hbar is the Planck constant). The tunnel probability is very small because of the smallness of Δ , itself an exponentially decreasing function of the spin ($S = 10$ in $\text{Mn}_{12}\text{-ac}$). At resonance, only a small fraction proportional to $P = \pi(\Delta/\hbar)^2/\gamma c$ of the SMM spins will tunnel whereas all the other spins will stay on their initial state $|S\rangle$ (with the probability $1 - P$), explaining why the steps in the hysteresis loop of Fig. 4 are finite, unlike the classical case where the magnetization reverses totally at a single switching field. This model gives a convincing interpretation of the persistence of “classical” hysteresis between quantum tunnelling resonances. However it remains qualitative because the effect of the environment is not taken into account.

The Prokof'ev and Stamp spin-bath model [8] gives a new view of mesoscopic tunnelling in the presence of a magnetic environment. In the simplest description, one can say that the levels of each molecule (Fig. 2 and 3) are shifted by small local dipolar fields that are diffe-

rent for each molecule. Each level of Fig. 2 and 3 is then replaced by a – relatively narrow – level density $N_{\downarrow}(\xi)$ with spin \downarrow on the left side of the barrier and $N_{\uparrow}(\xi)$ with spin \uparrow on the right side. Hyperfine and super-hyperfine interactions (also of dipolar origin) also play an important role. After each tunnelling spin reversal the “map” of the dipolar field distribution is modified with particularly strong modifications of local precession field axes of nuclear spins, inducing fast nuclear spin-spin motion at a time scale T_2 . The resulting tunnel probability can be written as [8]:

$$P_{\text{SB}}(\xi) = \Delta^2 e^{-|\xi|/\xi_0} N_{\uparrow}(\xi)/E_0 \quad (3)$$

where the “tunnel window” ξ_0 is given by the root mean square homogeneous distribution of hyperfine fields acting on a SMM, ξ is the applied bias field and E_0 is the energy associated with the nuclear spin-spin relaxation time T_2 . The Prokof'ev and Stamp tunnelling rate is by several orders of magnitude larger than the Landau-Zener one, showing that mesoscopic spin tunnelling is easily observable owing to the magnetic environment.

The zero-Kelvin results given above can readily be extended to finite temperatures to describe the “thermally activated tunnelling” regime mentioned above. At $T \geq T_c$ the spin-up density of states $m = S - n$, given by the Boltzmann law, is expressed as $N_{\uparrow}(\xi, n, T) = N_{\uparrow}(\xi) \exp[-(DS^2 - D(S - n)^2)/T]$, and the thermally activated tunnelling escape from this state will simply be given by (3) where $N_{\uparrow}(\xi)$ is replaced by $N_{\uparrow}(\xi, n, T)$ and $\Delta = \Delta_{s,-s}$ by $\Delta_{s-n,m'}$ where m' is the “landing” state. As the tunnel splitting increases exponentially when the spin state decreases ($\Delta_{s-n,m'} \gg \Delta_{s,-s}$), activated dynamic, becomes faster and hysteresis loops narrower (Fig. 4). Interestingly, the thermally activated form of (3) gives a quantum contribution to the exponential pre-factor of the classical Arrhenius law $1/\tau_0 \propto \Delta^2 e^{-|\xi|/\xi_0} N_{\uparrow}(\xi)/E_0$ where $\Delta \approx \Delta_{1,-1}$ (in zero-field).

In conclusion, the study of mesoscopic quantum tunnelling of spins led to the new field of “quantum dynamics of spins”, which extends towards complexity or simplicity. As an example, in the first case large molecules with $S = 30$ or nanoparticles with $S = 10^5$ may exhibit mesoscopic/macrosopic quantum tunnelling, whereas in the second case paramagnetic rare-earth ions show broad “classical” hysteresis loops with electro-nuclear co-tunnelling resonances at sub-Kelvin temperatures. In these studies the quantum dynamics is incoherent and tunnelling spin-reversal leads to “quantum relaxation” towards the phonon and spin

baths. Upon large separation of magnetic entities it has been possible to extend this relaxation regime to the “coherence” regime in which the time-dependent wavefunction of the SMM (or rare-earth) spins oscillates in time with phase preservation exceeding a microsecond [9]. This shows that in a microwave cavity robust entanglement between spins and photons can be achieved even with complex systems such as SMMs with huge full Hilbert spaces. Another extension of this field consists in studying a single SMM (such as $\text{Mn}_{12}\text{-ac}$) by coherent transport measurements through the molecule. Although significant progress has been achieved during these last years much remains to be done in this merger of quantum spin dynamics with spintronics (Fert and Grünberg).

References

- [1] E. Schrödinger, *Die Naturwissenschaften* **23**, 807, 823, 844 (1935), translation: J. D. Trimmer, *Proc. Amer. Philos. Soc.* **124**, 323 (1980)
- [2] A. J. Leggett, *J. Phys. (Paris), Colloq.* **39**, C6-1264 (1978)
- [3] M. Uehara, and B. Barbara, *J. Physique* **47**, 235 (1986). See also K. Ziemelis, *Nature milestones, spin*, S19 (2008), doi: 10.1038/nphys877
- [4] T. Lys, *Acta. Crystallogr. B* **36**, 2042 (1980)
- [5] R. Sessoli, D. Gatteschi, A. Caneschi, and M. A. Novak, *Nature* **365**, 141 (1993)
- [6] L. Thomas, F. Lioni, R. Ballou, D. Gatteschi, R. Sessoli, and B. Barbara, *Nature* **383**, 145 (1996). See also B. Barbara et al, *J. Mag. Mag. Mat.* **140**, 1825 (1995)
- [7] J. R. Friedman, M. Sarachik, J. Tejada, J. Maciejewski, and R. Ziolo, *Phys. Rev. Lett.* **76**, 20 (1996)
- [8] N. V. Prokof'ev, and P. C. E. Stamp, *Rep. Prog. Phys.* **63**, 669 (2000)
- [9] S. Bertaina, S. Gambarelli, T. Mitra, B. Tsukerrlat, A. Müller, and B. Barbara, *Nature* **453**, 203 (2008) and S. Bertaina, S. Gambarelli, A. Tkachuck, I.M. Kurkin, B. Malkin, A. Stepanov, and B. Barbara, *Nature Nanotechnol.* **2**, 39 (2007)

THE AUTHOR

Bernhard Barbara (at the prize ceremony with the president of the Société Française de Physique, Michèle Leduc, and DPG president Eberhard Umbach) studied physics in Grenoble and spent his whole career at the CNRS where he is now Directeur de Recherche. He is a pioneer in the field of mesoscopic magnetic systems and one of the most creative solid-state physicists in France.

